

# Anomalous Diffusion in a Dynamical Optical Lattice

Wei Zheng and Nigel R. Cooper

*T.C.M. Group, Cavendish Laboratory, J. J. Thomson Avenue, Cambridge CB3 0HE, United Kingdom*

(Dated: 12 Sep, 2017)

Motivated by experimental progress in strongly coupled atom-photon systems in optical cavities, we study theoretically the quantum dynamics of atoms coupled to a one-dimensional dynamical optical lattice. The dynamical lattice is chosen to have a period that is incommensurate with that of an underlying static lattice, leading to a dynamical version of the Aubry-André model which can cause localization of single-particle wavefunctions. We show that atomic wavepackets in this dynamical lattice generically spread via anomalous diffusion, which can be tuned between super-diffusive and sub-diffusive regimes. This anomalous diffusion arises from an interplay between quantum localization and quantum fluctuations of the cavity field.

One of the most interesting directions of research in coherent quantum systems concerns the collective dynamics of coupled atom-photon ensembles. Such situations arise for cold atomic gases in optical cavities[1] or waveguides[2, 3], where strong coupling between atomic motion and a photon field can be achieved. Coupling cold atoms even to a single cavity mode can dramatically change the steady state of the atomic gas[4–25] and lead to interesting nonequilibrium dynamics[26–36].

A transversely pumped Bose-Einstein condensate in a single-mode cavity can undergo a phase transition into a self-organized “superradiant” state, in which the cavity mode becomes highly occupied and generates a cavity-induced superlattice potential on the atoms. For current experiments[8, 9] this dynamical cavity-induced superlattice is commensurate with an underlying static optical lattice, therefore giving rise to a supersolid phase with extended Bloch waves. However, one can readily envisage situations in which the cavity-induced superlattice is incommensurate with the underlying static lattice. This leads to the interesting possibility that the cavity-induced superlattice leads to localization of the single-particle states. Indeed, several theoretical works have studied the steady state of cold atoms in such settings [50–52], and have found a self-organized localization-delocalization transition within a mean-field approximation.

In this paper, we show that the motion of atoms in a cavity-induced incommensurate lattice is qualitatively affected by the quantum fluctuations of the cavity field, leading to long-time behaviour that is not captured by mean-field theories. Specifically, we show that the atomic motion exhibits anomalous diffusion, in which the width of the wavepacket  $\sigma$  grows with time as  $\sigma \sim t^\gamma$  with  $0 < \gamma < 1$ . Anomalous diffusion exists widely in both classical and quantum systems. In classical random walks, anomalous diffusion is mostly associated with the failure of the central limit theorem and the presence of long-tailed distributions[39–41]. On the other hand, in closed quantum systems, anomalous diffusion is typically connected to the multifractal nature of eigenstates[44, 45]. Quantum anomalous diffusion is also predicted close to

many body localization[48, 49]. Due to the cavity loss, our dynamical lattice is an open system, so this anomalous diffusion cannot be explained by multifractal eigenstates. Instead, using the quantum trajectory picture, we show that the dynamics can be viewed as a form of Lévy walk with rests[46, 47]. This explanation relies both on quantum fluctuations of the cavity field and on quantum localization in the incommensurate potential, so is an inherently quantum phenomenon. We predict that evidence of this anomalous transport can be found in long-tailed distributions of photon correlations in the cavity field.

*Model.* We consider spinless atoms trapped by an optical lattice in a high-Q cavity (Fig. 1), both aligned along the  $x$ -direction. Two counterpropagating pump lasers are shone on the atom cloud from the  $z$ -direction. Denoting the cavity field operator by  $\hat{a}$ , the net potential on the atoms is  $V = A \cos^2(k_o x) + B \hat{a}^\dagger \hat{a} \cos^2(k_c x + \phi) + C(\hat{a} + \hat{a}^\dagger) \cos(k_p z) \cos(k_c x + \phi)$ . Here  $A$  is proportional to the optical lattice intensity,  $B$  is the cavity-atom coupling strength ( $\phi$  controls the relative positions of the optical lattice and the cavity mode), and  $C$  is the pump-cavity coupling proportional to the amplitude of the pump laser. We consider the transverse confinement to be sufficiently large that the transverse motion is frozen out. For deep enough lattices, we obtain a one dimensional tight-binding model as

$$H = \Delta \hat{a}^\dagger \hat{a} - J \sum_{j=1}^L \left( \hat{c}_{j+1}^\dagger \hat{c}_j + h.c. \right) + \lambda (\hat{a} + \hat{a}^\dagger) \sum_{j=1}^L u_j \hat{c}_j^\dagger \hat{c}_j + U \hat{a}^\dagger \hat{a} \sum_{j=1}^L u_j^2 \hat{c}_j^\dagger \hat{c}_j, \quad (1)$$

where  $\hat{c}_j^{(\dagger)}$  are the atomic field operators on lattice site  $j$ ;  $\Delta = \omega_c - \omega_p$  is the detuning of the cavity mode;  $u_j = \cos(2\pi\beta j + \phi)$ ,  $\beta = k_c/2k_o$ ;  $U$  and  $\lambda$  are the projections of  $B$  and  $C$  onto the Wannier functions. We have ignored interactions between atoms, as can be realized by a Feshbach resonance for bosons or for spinless fermions with contact interactions. Due to the leaking of photons from the cavity, the system should be described by the

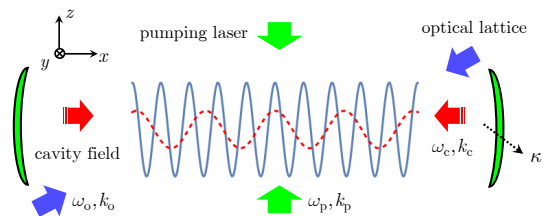


FIG. 1: Schematic diagram of the experimental setup. Atoms in an optical lattice and a standing wave cavity is driven by a transverse laser. The frequency  $\omega_p$  of the pump laser is far detuned from the atomic transition line but close to the cavity mode frequency  $\omega_c$ .

quantum master equation

$$\partial_t \rho = -i[H, \rho] + \kappa(2\hat{a}\rho\hat{a}^\dagger - \hat{a}^\dagger\hat{a}\rho - \rho\hat{a}^\dagger\hat{a}), \quad (2)$$

where  $2\kappa$  is the loss rate of the cavity photons.

If the cavity were directly driven by another pump laser, such that the cavity field is a coherent state  $\hat{a} \rightarrow \alpha$ , then the particles would experience a static effective potential  $V_{\text{eff}}(\alpha) = \sum_{j=1}^L [2\lambda \text{Re}(\alpha)u_j + U|\alpha|^2 u_j^2] \hat{c}_j^\dagger \hat{c}_j$ . In the case where  $\beta$  is an irrational number and  $U = 0$ , this reproduces the celebrated Aubry-André model, which exhibits a delocalization-localization transition for all the eigenstates[53]. Even when  $U \neq 0$ , this transition still survives, but now with mobility edges in the energy spectrum[54]. We are interested in cases without this direct drive, in which the cavity has its own quantum dynamics and the atoms feel a dynamical potential.

*Mean field steady state.* From Eq. (2), one finds that the mean cavity field  $\alpha(t) = \langle \hat{a}(t) \rangle$  evolves as  $i\partial_t \alpha = (\Delta - i\kappa + UR)\alpha + \lambda\Theta$ , where  $\Theta = \sum_j u_j \langle \hat{c}_j^\dagger \hat{c}_j \rangle$ , and  $R = \sum_j u_j^2 \langle \hat{c}_j^\dagger \hat{c}_j \rangle$ . We seek a steady state in which  $\partial_t \alpha = 0$  and find  $\alpha = -\frac{\lambda\Theta}{\Delta - i\kappa + UR}$ . The expectation value  $\langle \hat{c}_j^\dagger \hat{c}_j \rangle$  can be obtained from the ground state of the mean field Hamiltonian in which the atoms experience the effective potential  $V_{\text{eff}}(\alpha)$ .

We consider one atom in the cavity, and numerically obtain the steady state phase diagram, see Fig. 2. To describe the localization of the particle, we calculate the inverse participation ratio in real space of the atomic wavefunction,  $p = \sum_{j=1}^L \left| \langle \hat{c}_j^\dagger \hat{c}_j \rangle \right|^2$ . One notes that highly localized density gives  $p \sim 1$ ; while an extended wavefunction has  $p \sim 1/L$ .

In the weak pumping regime, the system is in the “normal” phase, which has no superradiance,  $\alpha = 0$ , and the effective potential vanishes,  $V_{\text{eff}}(\alpha) = 0$ . So the atomic states are delocalized. When  $U$  is large, as the pumping strength increases, the system undergoes a second order phase transition from the “normal” phase to a “delocalized superradiant” phase, see Fig. 2(b). As a result the effective potential  $V_{\text{eff}}(\alpha)$  is non-zero, and the atomic

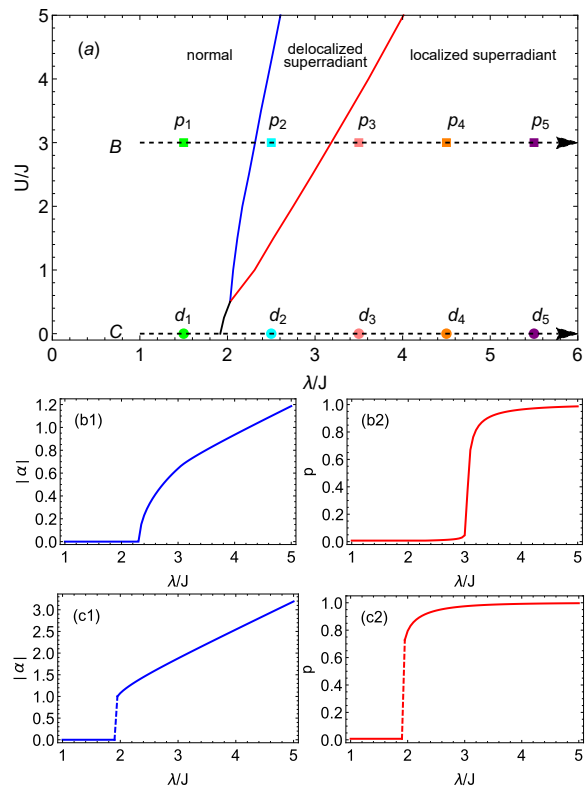


FIG. 2: (a) Phase diagram of mean field steady state. (b1), (b2) Second order phase transition along the line B in (a). (b1) Mean cavity field  $\alpha$ . (b2) Inverse participation ratio in real space  $p$ . (c1), (c2) First order phase transition along the line C in (a). Here  $L = 201$ ,  $\beta = (\sqrt{5} - 1)/2$ ,  $\phi = \pi/2$ ,  $\Delta/J = 1$ , and  $\kappa/J = 1.2$ . The square dots,  $p_i$  ( $i = 1, \dots, 5$ ), represent the pumping strengths  $\lambda/J = 1.5, 2.5, 3.5, 4.5, 5.5$ , respectively, and  $U/J = 3$ ; while the circle dots  $d_i$  have the same pumping strengths but with  $U/J = 0$ .

density is modulated but still delocalized. For larger pumping strength, the system undergoes a transition into a “localized superradiant” phase. In this phase, the effective potential becomes so large that the atomic wavefunction is localized. In the small  $U$  regime, these two transitions merge into one first order transition, where the cavity field and the effective potential suddenly jump to large values [Fig. 2(c)]. Note that these conclusions are also valid for the  $N$  boson system, with the same phase diagram unchanged provided we keep  $\lambda/J$ ,  $U/J$  invariant and scale  $\Delta/J \rightarrow N\Delta/J$ ,  $\kappa/J \rightarrow N\kappa/J$ . The appearance of a localized superradiant phase is consistent with a previous study[52].

*Wavepacket spreading.* Given the fact that the cavity can drive a transition between extended and localized states, at least at mean-field level, it is natural to ask how this affects the particle *transport*. To answer that, we have investigated how an atomic wave packet spreads in the driven and damped cavity field. We set the initial state to be the atom located in the centre of the

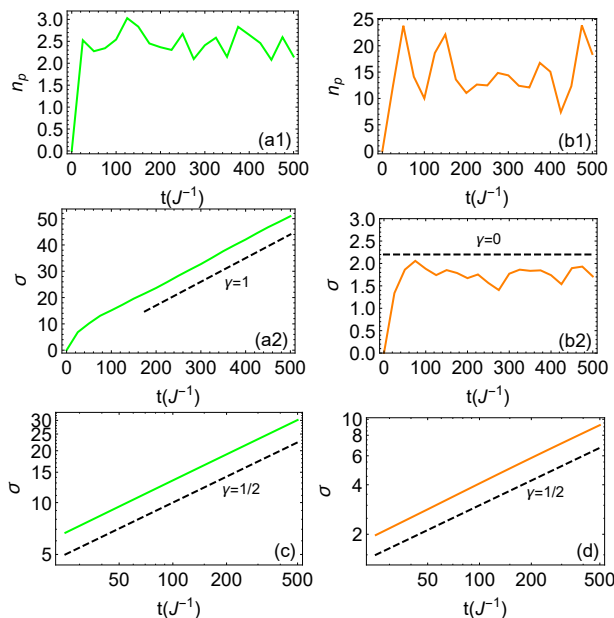


FIG. 3: (a1), (a2) Dissipationless nonequilibrium dynamics in the delocalized regime. (a1) The photon number  $n_p$ , (a2) wave packet width  $\sigma$ . The dashed line is a guide for ballistic behaviour  $\gamma = 1$ . (b1), (b2) Dissipationless nonequilibrium dynamics in the localized regime. (c), (d) Dynamics in the large dissipation limit in delocalized and localized phases of the mean-field model respectively. The dashed line is a guide for diffusion  $\gamma = 1/2$ . The parameters of (a1), (a2) and (c) are identical to the dots  $d_1$  in Fig. 2(a), while the parameters of (b1), (b2) and (d) are given by the dots  $d_4$  in Fig. 2(a).

lattice and the cavity empty. We then consider turning on the pump laser, and calculate the time evolution of the wave packet width  $\sigma(t) = \sqrt{\langle X^2 \rangle - \langle X \rangle^2}$ , where  $X = \sum_j j \hat{c}_j^\dagger \hat{c}_j$  is the centre-of-mass of the wave packet. We find, quite generally, that the width grows as a power-law,  $\sigma(t) \sim t^\gamma$  at long times. However, the nature of this growth is a surprisingly subtle issue: its qualitative form requires an accurate description of the quantum fluctuations of the driven-damped cavity field. We illustrate this by first presenting results for two limiting cases of the cavity damping (for these cases we set  $U = 0$  for simplicity).

*Dissipationless limit.* We first consider the dissipationless limit,  $\kappa = 0$ . The system is then closed and the dynamics is given by unitary evolution under the Hamiltonian (1). We numerically simulate the unitary evolution process, obtaining the photon number  $n_p(t) = \langle \hat{a}^\dagger \hat{a} \rangle$  and the wave packet width  $\sigma(t)$ , see Fig. 3. The photon number first rises from zero to a nonzero value in a short time, and then shows large fluctuations around this nonzero value. For small pumping strength, the average photon number is small and the wave packet spreading is ballistic,  $\gamma = 1$  [Fig. 3(a1)(a2)]. While for large pumping strength, the photon number is larger and the width

finally saturates at long times, indicating localized behaviour,  $\gamma = 0$  [Fig. 3(b1)(b2)]. These qualitative forms of dynamics are consistent with the mean field steady states: at small coupling the steady state wave function is delocalized; while at large couplings, the steady state wave function is localized.

*Large dissipation limit.* We now consider the opposite limit, in which the dissipation  $\kappa$  is so large that the lifetime of the cavity is negligible. In this case, the cavity field will adiabatically follow the distribution of the atom density, with  $\hat{a} \approx -\frac{\lambda}{\Delta - i\kappa} \hat{K}$ , where  $\hat{K} = \sum_j u_j \hat{c}_j^\dagger \hat{c}_j$ . Since the cavity field is fixed by the atomic density, one can substitute this formula into the Hamiltonian (1) and the quantum master equation (2) to obtain the effective master equation for the atom as  $\partial_t \rho_a = -i [H_{\text{eff}}, \rho_a] + \kappa' \left( 2\hat{K} \rho_a \hat{K} - \hat{K}^2 \rho_a - \rho_a \hat{K}^2 \right)$ . Here  $\rho_a$  is the reduced density matrix of the atoms, and the effective Hamiltonian is  $H_{\text{eff}} = -J \sum_{j=1}^L \left( \hat{c}_{j+1}^\dagger \hat{c}_j + h.c. \right) + V' \sum_{j=1}^L u_j^2 \hat{c}_j^\dagger \hat{c}_j$ , with  $V' = -\frac{2\lambda^2 \Delta}{\Delta^2 + \kappa^2}$  and  $\kappa' = \frac{\lambda^2 \kappa}{\Delta^2 + \kappa^2}$ . This effective model describes an atom hopping in a quasi-periodic lattice with a global noise, which is imposed by the damped cavity field. We have numerically solved this effective quantum master equation. The temporal dynamics of the width of the atomic wave packet is shown Fig. 3(b). We find that, in this large dissipation limit, the wavepacket always spreads diffusively  $\sigma \sim t^{1/2}$ , both where the mean-field solution shows delocalized [Fig. 3(c)] and localized [Fig. 3(d)] behaviours. Thus, this global noise destroys the coherence and makes the atom diffuse like a classical Brownian particle at long times.

*Quantum trajectory method.* After considering these two limiting cases, we now investigate the generic situation, in which the cavity dissipation is finite. We employ the so-called quantum trajectory method[56], which is a stochastic way to simulate the quantum master equation by averaging over many quantum trajectories.

We have used this method to simulate the wave packet spreading for different pumping strengths. The results are plotted in Fig. 4. In Fig. 4(a), one can see a typical dynamics of the system. Similar to the dissipationless limit, the photon number rises to a nonzero value in a short time scale. After that, the cavity field enters into a quasi-steady state, in which the photon number has small fluctuations around its mean. Note that the fluctuation amplitude is much smaller than that in the dissipationless limit [Fig. 3(a1)], as the existence of the cavity dissipation suppresses these fluctuations. At short times, the width of the wave packet grows quickly from zero, since the cavity field has not yet built up a large effective potential. However, at long times, after the cavity field has reached its quasi-steady state, we find that the wave packet spreads according to anomalous diffusion,  $\sigma \sim t^\gamma$ , with  $0 < \gamma < 1$ . We find that the exponent  $\gamma$  depends on

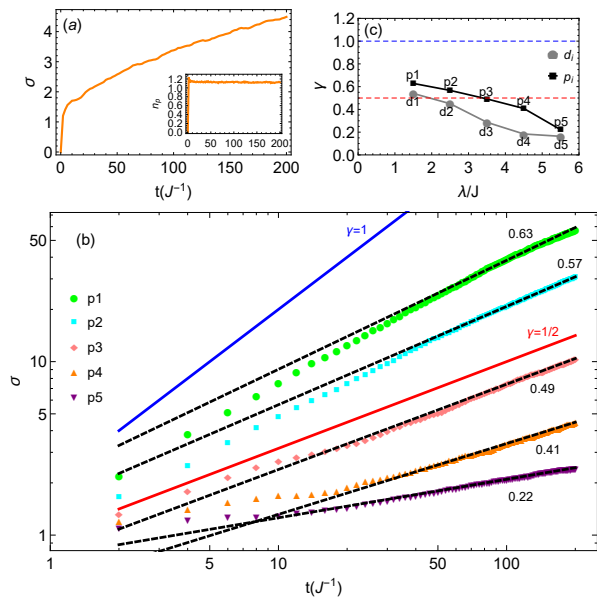


FIG. 4: (a) Photon number and wave packet width evolution from the exact quantum trajectory method. The parameters are given by the point  $p_4$  in Fig. 2(a). (b) Evolution of the wave packet width. Dashed lines are the results of fitting to  $\sigma = at^\gamma$ , and the corresponding numbers are the exponents. The two solid lines represent the ballistic,  $\gamma = 1$ , and diffusive,  $\gamma = 1/2$ , cases. (c) The exponent  $\gamma$  crosses over from super-diffusion to sub-diffusion with increasing pump strength. The two dashed lines show the ballistic and diffusive values. The parameters of  $d_i$  and  $p_i$  can be found in Fig. 2(a).

the pumping strength and other parameters. As shown in Fig. 4(b), when the pumping strength is small,  $\gamma$  is relatively large, corresponding to super-diffusion,  $\gamma > 1/2$ . When the pumping strength is large,  $\gamma$  becomes relatively small, crossing over to the sub-diffusion regime,  $\gamma < 1/2$  [see Fig. 4(c)]. This behaviour is very different from the dissipationless and large dissipation limits. This indicates that the observed anomalous diffusion is a result of both the dissipation and the cavity dynamics.

How can we understand this anomalous diffusion? We plot the evolution of the photon number and the wave packet width for a single quantum trajectory in Fig. 5. Comparing the photon number and the width, one finds that when the photon number is large the width almost does not grow: at these times, the effective potential induced by the cavity is very strong, such that the wave packet is localized and cannot spread freely. When the cavity field fluctuates to a small value, it reduces the effective potential: at these times, the wave packet can spread ballistically until the revival of the photon number. With the help of this picture, we can map the particle hopping into a Lévy walk with rests[46, 47]. When the cavity field is lower than a threshold, the particle moves ballistically at a certain maximal velocity set by the bandwidth. When the cavity field exceeds the

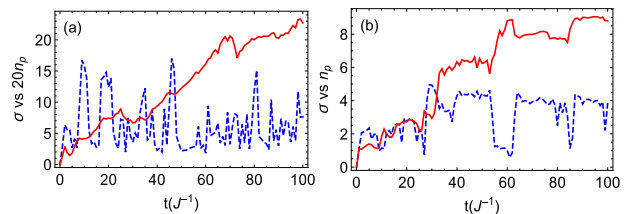


FIG. 5: Individual quantum trajectories of the stochastic evolution in: (a) the super-diffusive regime; and (b) the sub-diffusive regime. The solid line is the wave packet width, and the dashed line is the photon number [multiplied by 20 in (a)]. The parameters of (a) and (b) are given by the dots  $d_1$  and  $d_3$  in Fig. 2(a).

threshold, due to the quantum localization the motion is switched off, and the particle is at rest. The time interval of the “on” and “off”, i.e. moving time and waiting time are random variables, since the cavity is affected by the noise from the environment. Crucially, we find that, in the large pumping regime, the distribution of waiting times has a broad tail, leading to subdiffusive behaviour. While in the small pumping regime, the broad tail of the moving time distribution dominates, and gives superdiffusion. By increasing the pump strength, one increases the mean cavity field and decreases the switching threshold. This gradually tunes the distribution of waiting time and the moving time, resulting in a crossover from sub-diffusion to superdiffusion.

*Final remarks.* Anomalous diffusion is predicted in other quantum systems with specific forms of coloured noise[57–60]. In our model anomalous diffusion arises naturally in a very simple experimental setting with generic form of damping. The wave packet spreading could be detected by situ imaging. However, the anomalous properties could also be detected from the photons leaking from the cavity[28] for which we predict long-tailed distributions of lower and higher cavity occupations. It will be interesting to consider situations in higher dimensions, or for larger particle densities in which cavity-mediated interactions will also play a role.

This work was supported by EPSRC Grant Nos. EP/K030094/1 and EP/P009565/1.

- 
- [1] H. Ritsch, P. Domokos, F. Brennecke, and T. Esslinger, Rev. Mod. Phys. **85**, 553 (2013).
  - [2] J. D. Thompson, T. G. Tiecke, N. P. de Leon, J. Feist, A. V. Akimov, M. Gullans, A. S. Zibrov, V. Vuletić, and M. D. Lukin, Science **340**, 1202 (2013).
  - [3] A. Goban, C. -L. Hung, S. -P. Yu, J. D. Hood, J. A. Muniz, J. H. Lee, M. J. Martin, A. C. McClung, K. S. Choi, D. E. Chang, O. Painter, and H. J. Kimble, Nat. Commun. **5**, 3808 (2014).
  - [4] K. Baumann, C. Guerlin, F. Brennecke, and T. Esslinger, Nature (London) **464**, 1301 (2010).

- [5] R. Mottl, F. Brennecke, K. Baumann, R. Landig, T. Donner, T. Esslinger, *Science* **336**, 1570 (2012).
- [6] R. Landig, F. Brennecke, R. Mottl, T. Donner, T. Esslinger, *Nat. Commun.* **6**, 7046 (2015).
- [7] M. R. Bakhtiari, A. Hemmerich, H. Ritsch, and M. Thorwart, *Phys. Rev. Lett.* **114**, 123601 (2015).
- [8] J. Klinder, H. Keßler, M. R. Bakhtiari, M. Thorwart, and A. Hemmerich, *Phys. Rev. Lett.* **115**, 230403 (2015).
- [9] R. Landig, L. Hruby, N. Dogra, M. Landini, R. Mottl, T. Donner and T. Esslinger, *Nature (London)* **532**, 476 (2016).
- [10] P. Domokos and H. Ritsch, *Phys. Rev. Lett.* **89**, 253003 (2002).
- [11] D. Nagy, G. Kónya, G. Szirmai, and P. Domokos, *Phys. Rev. Lett.* **104**, 130401 (2010).
- [12] M. J. Bhaseen, M. Hohenadler, A. O. Silver, and B. D. Simons, *Phys. Rev. Lett.* **102**, 135301 (2009).
- [13] S. Gopalakrishnan, B. L. Lev, and P. M. Goldbart, *Phys. Rev. A* **82**, 043612 (2010).
- [14] J. Keeling, M. J. Bhaseen, and B. D. Simons, *Phys. Rev. Lett.* **112**, 143002 (2014).
- [15] F. Piazza, and P. Strack, *Phys. Rev. Lett.* **112**, 143003 (2014).
- [16] Y. Chen, Z. Yu, and H. Zhai, *Phys. Rev. Lett.* **112**, 143004 (2014).
- [17] Y. Deng, J. Cheng, H. Jing, and S. Yi, *Phys. Rev. Lett.* **112**, 143007 (2014).
- [18] L. Dong, L. Zhou, B. Wu, B. Ramachandhran, and H. Pu, *Phys. Rev. A* **89**, 011602 (2014).
- [19] Y. Chen, H. Zhai, and Z. Yu, *Phys. Rev. A* **91**, 021602 (2015).
- [20] J.-S. Pan, X.-J. Liu, W. Zhang, W. Yi, and G.-C. Guo, *Phys. Rev. Lett.* **115**, 045303 (2015).
- [21] G. Szirmai, G. Mazzarella, and L. Salasnich, *Phys. Rev. A* **91**, 023601 (2015).
- [22] C. Kollath, A. Sheikhan, S. Wolff, and F. Brennecke, *Phys. Rev. Lett.* **116**, 060401 (2016).
- [23] Y. Chen, Z. Yu, and H. Zhai, *Phys. Rev. A* **93**, 041601 (2016).
- [24] A. Sheikhan, F. Brennecke, C. Kollath, *Phys. Rev. A* **93**, 043609 (2016).
- [25] N. Dogra, F. Brennecke, S.D. Huber, T. Donner, *Phys. Rev. A* **94**, 023632 (2016).
- [26] F. Brennecke, S. Ritter, T. Donner, and T. Esslinger, *Science* **322**, 235 (2008).
- [27] J. Klinder, H. Keßler, M. Wolke, L. Mathey, and A. Hemmerich, *PNAS* **112**, 3290 (2015).
- [28] H. Keßler, J. Klinder, B. P. Venkatesh, Ch. Georges, and A. Hemmerich, arXiv: 1606.08386.
- [29] C. Maschler, H. Ritsch, *Phys. Rev. Lett.* **95**, 260401 (2005).
- [30] J. Keeling, M. J. Bhaseen, and B. D. Simons, *Phys. Rev. Lett.* **105**, 043001 (2010).
- [31] G. Kónya, G. Szirmai, D. Nagy, and P. Domokos, *Phys. Rev. A* **89**, 051601(R) (2014).
- [32] M. Kulkarni, B. Öztop, and H. E. Türeci, *Phys. Rev. Lett.* **111**, 220408 (2013).
- [33] S. Schutz and G. Morigi, *Phys. Rev. Lett.* **113**, 203002 (2014).
- [34] F. Piazza and H. Ritsch, *Phys. Rev. Lett.* **115**, 163601 (2015).
- [35] W. Zheng and N. R. Cooper, *Phys. Rev. Lett.* **117**, 175302 (2016).
- [36] S. Wolff, A. Sheikhan, and C. Kollath, *Phys. Rev. A* **94**, 043609 (2016).
- [37] Y. Sagi, M. Brook, I. Almog, and N. Davidson, *Phys. Rev. Lett.* **108**, 093002 (2012).
- [38] C. D’Errico, M. Moratti, E. Lucioni, L. Tanzi, B. Deissler, M. Inguscio, G. Modugno, M. B. Plenio, and F. Caruso, *New J. Phys.* **15**, 045007 (2013).
- [39] R. Metzler, E. Barkai, and J. Klafter, *Phys. Rev. Lett.* **82**, 3563 (1999).
- [40] R. Metzler and J. Klafter, *Phys. Rep.* **339**, 1 (2000).
- [41] I. M. Sokolov and J. Klafter, *Chaos* **15**, 26103 (2005).
- [42] P. Levy, *Bull. la Société Mathématique Fr.* **67**, 1 (1939).
- [43] F. Bardou, J. Bouchaud, A. Aspect, and C. Cohen-Tannoudji, *Lévy Statistics and Laser Cooling* (Cambridge University Press, Cambridge, England, 2002).
- [44] F. Piéchon, *Phys. Rev. Lett.* **76**, 4372 (1996).
- [45] S. Roy, I. M. Khaymovich, A. Das, and R. Moessner, arXiv: 1706.05012.
- [46] V. Zaburdaev, S. Denisov, and J. Klafter, *Rev. Mod. Phys.* **87**, 483 (2015).
- [47] J. Klafter and I. M. Sokolov, *First Steps in Random Walks*, (Oxford University Press, New York, 2011).
- [48] K. Agarwal, S. Gopalakrishnan, M. Knap, M. Müller, and E. Demler, *Phys. Rev. Lett.* **114**, 160401 (2015).
- [49] Y. B. Lev, I. D. M. Kennes, C. Klöckner, D. R. Reichman, and C. Karrasch, arXiv: 1702.04349v1.
- [50] L. Zhou, H. Pu, K. Zhang, X. Zhao, and W. Zhang, *Phys. Rev. A* **84**, 043606 (2011).
- [51] H. Habibian, A. Winter, S. Paganelli, H. Rieger, and G. Morigi, *Phys. Rev. Lett.* **110**, 075304 (2013).
- [52] K. Rojan, R. Kraus, T. Fogarty, H. Habibian, A. Minguzzi, and G. Morigi, *Phys. Rev. A* **94**, 013839 (2016).
- [53] S. Aubry and G. André, *Ann. Isr. Phys. Soc.* **3**, 133 (1980).
- [54] J. Biddle and S. Das Sarma, *Phys. Rev. Lett.* **104**, 070601 (2010).
- [55] S. Diehl, W. Yi, A. J. Daley, and P. Zoller, *Phys. Rev. Lett.* **105**, 227001 (2010).
- [56] A. J. Daley, *Adv. Phys.* **63**, 77 (2014).
- [57] H. Grabert, P. Schramm and G. Ingold, *Phys. Rev. Lett.* **58**, 1285 (1987).
- [58] G. W. Ford and R. F. O’Connell, *Phys. Rev. A* **73**, 032103 (2006).
- [59] N. V. Prokof’ev, and P. C. E. Stamp, *Phys. Rev. A* **74**, 020102(R) (2006).
- [60] E. Gholami, and Z. M. Lashkani, *Phys. Rev. E* **95**, 022216 (2017).